Catalysis Communications 16 (2011) 124–127

Contents lists available at SciVerse ScienceDirect

Catalysis Communications

journal homepage: www.elsevier.com/locate/catcom

Short Communication

Unexpected methanol-to-olefin conversion activity of low-silica aluminophosphate molecular sieves ☆

Weili Dai [a,b], Niu Li [a], Landong Li [a,*], Naijia Guan [a], Michael Hunger [b,*]

[a] Key Laboratory of Advanced Energy Materials Chemistry (Ministry of Education), College of Chemistry, Nankai University, Tianjin 300071, P.R. China
[b] Institute of Chemical Technology, University of Stuttgart, D-70550 Stuttgart, Germany

ARTICLE INFO

Article history:
Received 27 July 2011
Received in revised form 15 September 2011
Accepted 21 September 2011
Available online 29 September 2011

Keywords:
Methanol-to-olefin conversion
Aluminophosphate molecular sieves
Brønsted acid sites
Hydrocarbon pool compounds

ABSTRACT

Low-silica AlPO-18, AlPO-34, and AlPO-41 with Brønsted site densities of 0.006 to 0.014 mmol/g have been applied as methanol-to-olefin (MTO) conversion catalysts. At 673 K, AlPO-18 and AlPO-34 are active, while AlPO-41 did not exhibit obvious MTO activity. In situ UV/Vis spectroscopy of working AlPO-18 and AlPO-34 shows bands of aromatic compounds, but no formation of these species was found for AlPO-41 with one-dimensional 10-ring pores. This study indicates that the MTO reaction over aluminophosphates requires a minimum Brønsted site density and a suitable framework topology with cages like in AlPO-18 and AlPO-34 allowing the formation and stabilization of aromatics.

1. Introduction

The methanol-to-olefin (MTO) conversion over solid acid catalysts has received great attention in the past decades as an alternative route for the production of light olefins from non-oil sources [1]. A variety of acidic microporous catalysts have been studied as MTO catalysts [2–6]. Generally, the acidity and topology are two key factors controlling the catalytic performances of these materials. For a given MTO catalyst with defined topology, Brønsted acid sites play a vital role in the MTO conversion. On one side, the Brønsted acid sites facilitate the formation of aromatics and cyclic carbenium ions during an induction time, which then act as hydrocarbon pool species on the working catalyst [7–9]. On the other side, coke compounds, i.e. large polycyclic aromatics, are formed at Brønsted acid sites with further progress of the reaction and eventually cause catalyst deactivation [10,11].

Since SAPO-34 with large cages and small 8-ring windows is reported to be a very promising catalyst for the MTO reaction, many researches have been focused on the effect of Brønsted acidity on the catalytic performances of this material [12–14]. For example, controlled decrease of the Brønsted site density of SAPO-34 by reducing the silicon content in the synthesis or post-synthetic silanation and disilanation is useful to increase the olefin/alkane ratio as well as to decrease the coke formation [12,13]. Hence, the question arises, what will happen if most of the Brønsted acid sites in SAPO catalysts are eliminated.

The aim of the present work is to clarify whether the MTO reaction can be performed over aluminophosphate-type molecular sieves possessing CHA (AlPO-34), AEI (AlPO-18), and AFO (AlPO-41) topologies and with very low numbers of Brønsted acid sites. Furthermore, the effect of the framework topology of these molecular sieves on the MTO reaction was studied.

2. Experimental

2.1. Synthesis of aluminophosphates

All the aluminophosphate-type zeolites were synthesized via hydrothermal methods following the procedures described in literature [15–17] using pseudo-boehmite as aluminum source containing traces of silicon. The chemical compositions of the synthetic mixtures and the synthesis conditions of aluminophosphates are summarized in Table S1 (Supporting information). The as-synthesized materials were heated with a rate of 2 K/min to 973 K in a muffle oven under flowing synthetic air (60 l/h, 20 vol.% oxygen) for 4 h until complete removal of the occluded organic templates.

2.2. Characterization of aluminophosphate catalysts

X-ray diffraction (XRD) patterns of the samples were recorded on a Bruker D8 diffractometer with Cu Kα radiation (λ = 1.5418 Å) from 5 to 50° with a scan speed of 6.0°/min. The surface areas of the

☆ This work was presented on the Vietnam–German Conference on Catalytical and Chemical Technology for Sustainable Development in Hanoi, February 21–23, 2011, jointly organized by Vietnam Institute for Industrial Chemistry (VIIC), Hanoi University of Technology (HUT), Vietnam Petroleum Institute (VPI), Hanoi University of Sciences (HUS) and Leibniz-Institut für Katalyse (LIKAT) an der Universität Rostock, Germany.

* Corresponding authors. Tel./fax: +86 22 2350 0341.
E-mail addresses: lild@nankai.edu.cn (L. Li), michael.hunger@itc.uni-stuttgart.de (M. Hunger).

1566-7367/$ – see front matter © 2011 Elsevier B.V. All rights reserved.
doi:10.1016/j.catcom.2011.09.025

catalysts were obtained by means of nitrogen adsorption measurements performed at 77 K on a Quantachrome Autosorb 3B instrument. The chemical compositions of the calcined samples were determined by ICP-AES.

^{1}H MAS NMR spectra were recorded on a Bruker Avance III spectrometer. The samples used for the ^{1}H MAS NMR studies were dehydrated at 723 K in vacuum ($p<10^{-2}$ Pa) for 12 h. The determination of the number of accessible Brønsted acid sites was performed by adsorption of NH_3 at room temperature. After the NH_3 loading, the samples were evacuated at 453 K for 2 h to eliminate physisorbed ammonia. Quantitative ^{1}H MAS NMR measurements were performed by comparing the signal intensities of the samples under study with the intensity of an external intensity standard.

2.3. Catalytic investigations

The methanol conversion was performed in a fixed-bed flow microreactor at atmospheric pressure. Typically, 0.4 g sample (sieve fraction, 0.25–0.5 mm) was placed in a stainless steel reactor (5 mm i.d.) and activated under flowing N_2 at 723 K for 1 h. Methanol was injected with 0.5 ml/h (WHSV = 1/h) at 473 K. The reaction products were analyzed via an on-line gas chromatograph equipped with a flame ionization detector and a capillary column Plot Q to separate the C_1–C_8 hydrocarbons.

2.4. Characterization of occluded organic compounds on aluminophosphate catalysts

The composition of the hydrocarbon pool compounds formed under reaction conditions on the working catalysts was studied by in situ UV/Vis spectroscopy using an AvaSpec-2048 Fiber Optic spectrometer, an AvaLight-DH-S deuterium light source by Avantes, and a glass fiber reflection probe HPSUV1000A by Oxford Electronics. Reference UV/Vis spectra of silicoaluminophosphates were recorded at reaction temperature prior to starting the methanol flow. UV/Vis spectra were conducted at 200 to 600 nm in the diffuse reflection mode.

3. Results and discussion

3.1. Physico-chemical properties of the aluminophosphates under study

The XRD patterns of the aluminophosphate molecular sieves are shown in Fig. 1. Typical diffraction lines corresponding to AlPO-34 [15], AlPO-18 [16], and AlPO-41 [17] are observed, indicating that pure phases of the aforementioned framework topologies were obtained for the as-synthesized materials. The chemical composition and BET surface areas of the calcined samples are given in Table 1. The $n_{Si}/n_{(Si+Al+P)}$ ratios of AlPO-34, AlPO-18, and AlPO-41 are 0.01, 0.02, and 0.01, respectively, indicating that very small amounts of silicon are introduced into the aluminophosphate materials.

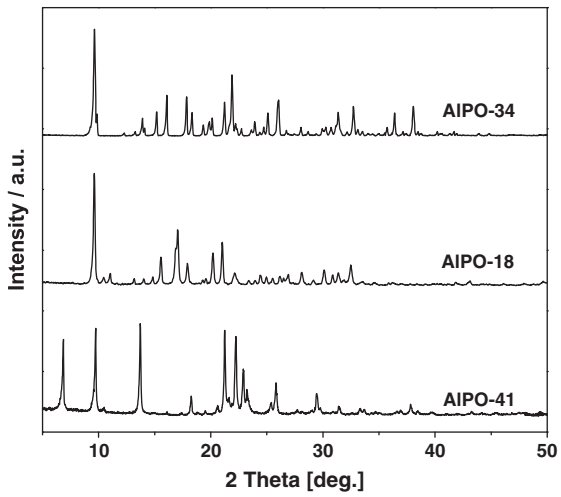

Fig. 1. XRD patterns of the aluminophosphate molecular sieves under study.

The Brønsted acid sites of the aluminophosphates under study were characterized by ^{1}H MAS NMR spectroscopy. The spectra shown in Fig. 2 consist of signals at 3.7 and 4.3 ppm, which are due to bridging OH groups (SiOHAl), i.e. Brønsted acid sites, in different local structures. Specifically, the signals at 3.7 ppm indicate the presence of SiOHAl groups in large cages and pores, while the signals at 4.3 ppm are assigned to SiOHAl groups in small structural building units [18,19]. Loading of ammonia on the aluminophosphates and subsequent desorption of the physisorbed probe molecules led to an ammonium signal at 6.4 ppm [18]. The residual weak signal at 3.7 ppm after the ammonia loading is due to non-accessible SiOHAl groups. For AlPO-34, AlPO-18, and AlPO-41, the numbers of accessible Brønsted acid sites were found to be 0.014, 0.006, and 0.008 mmol/g, respectively. Compared with the results of elemental analysis, this finding means that only a few of silicon atoms (less than 10%) caused a formation of bridging OH groups (SiOHAl). But it indicates that very small amounts of Brønsted acid sites were formed on aluminophosphates via introducing few silicon atoms in the framework. Additional signals at 0.5 to 0.9 ppm, which were observed before and after ammonia loading on aluminophosphates, are due to non-acidic POH and AlOH groups at framework defects and the crystal surfaces.

3.2. Catalytic performance of the aluminophosphate catalysts

The time dependence of the methanol conversion and product selectivity during the MTO conversion over the aluminophosphates under study is shown in Fig. 3. At 673 K, AlPO-34 exhibits 100% methanol conversion with more than 90% selectivity to C_2–C_4 olefins at a time-on-stream (TOS) of 7.5 h. After TOS = 10.5 h, the selectivity to C_2–C_4 olefins gradually decreased to ca. 50%, while the methanol conversion was ca. 95%. AlPO-18 also exhibits MTO activity, but catalytic performance is not as good as that of AlPO-34. Typically, 100% methanol conversion with 90% selectivity to C_2–C_4 olefins was observed after the initial TOS = 5 min. With the further extension of the reaction time, the selectivity to C_2–C_4 decreased gradually and finally dropped down to 40% after TOS = 10.5 h. AlPO-41, on the other hand, does not exhibit obvious MTO activity and dimethyl ether (DME) was the dominant product instead of light olefins during the methanol conversion. The catalytic results clearly indicate that the MTO reaction can be realized over AlPO-34 and AlPO-18 having traces of Brønsted acid sites. The different MTO property of AlPO-41 having a similar Brønsted site density like AlPO-18 must be considered in connection with the different framework topology (vide supra).

Table 1
Chemical compositions and surface areas of the calcined samples under study.

Samples	Elemental analysis [a] (mmol/g)				BET surface area [b] (m^2/g)	Brønsted acid sites [c] n_{acOH}/mmol g^{-1}
	n_{Al}	n_P	n_{Si}	$n_{Si}/(n_{Si}+n_{Al}+n_P)$		
AlPO-34	6.90	6.62	0.14	0.01	332	0.014
AlPO-18	5.61	5.56	0.18	0.02	400	0.006
AlPO-41	6.92	6.89	0.17	0.01	310	0.008

[a] Determined by ICP-AES.
[b] Determined by N_2-absorption.
[c] Determined by ^{1}H MAS NMR spectroscopy.

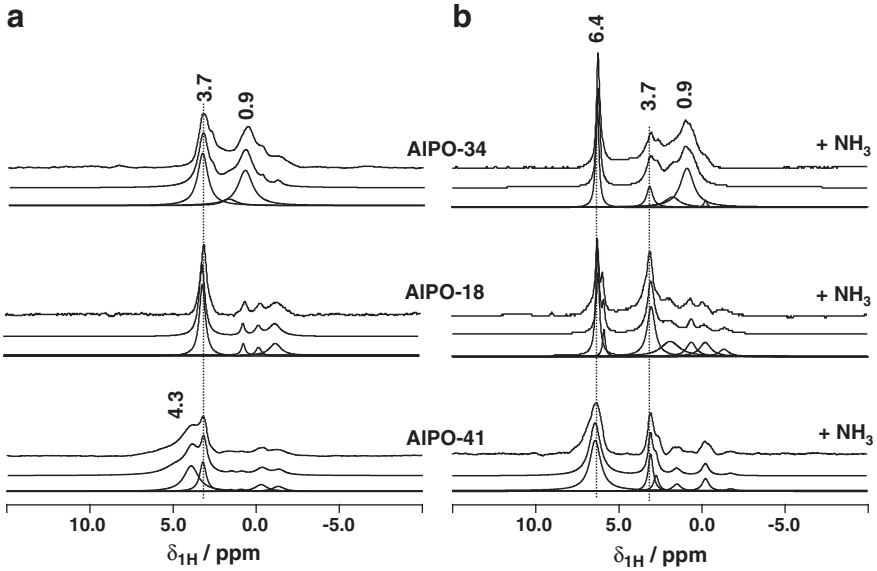

Fig. 2. ^{1}H MAS NMR spectra of calcined samples: (a) samples dehydrated at 673 K for 12 h, (b) samples like in (a), but after loading with NH_3 and evacuation at 453 K for 2 h.

3.3. In situ UV/Vis studies of the organic deposits formed during the MTO reaction

With in situ UV/Vis spectroscopy, the nature of olefinic and aromatic compounds formed during the MTO conversion was studied under reaction conditions. For AlPO-34, a weak band appeared at ca. 240 nm after the initial TOS = 5 min of the MTO reaction at 673 K indicating the rapid formation of dienes (Fig. 4) [20]. With the further progress of the MTO reaction, polyalkyl aromatics causing a band at ca. 270 nm and benzene-type carbenium ions responsible for a band at ca. 390 nm were formed [21]. For AlPO-18, UV/Vis bands of dienes, polyalkyl aromatics, and benzene-type carbenium ions were observed after TOS = 20 min during the MTO reaction, similar to those obtained for AlPO-34. However, the amounts of these species were much lower, probably due to the lower Brønsted site density available on AlPO-18 in comparison with AlPO-34. For AlPO-41, only traces of UV/Vis sensitive dienes (band at 240 nm) and polyalkyl aromatics (band at 270 nm) were observed after TOS = 20 min and no bands of benzene-type carbenium ions (ca. 390 nm) occurred.

3.4. Factors controlling the activity and selectivity of aluminophosphate catalysts

Generally, the acidity and the framework topology of molecular sieves are key factors controlling their catalytic performances in the MTO reaction [22]. In the present study, the MTO conversion could be realized over AlPO-34 as well as AlPO-18 with better methanol conversions and C_1–C_4 selectivities over AlPO-34 than over AlPO-18 under same reaction conditions.

AlPO-34 and AlPO-18 both possess very similar three-dimensional cages interconnected by 8-ring windows, while AlPO-41 possesses large one-dimensional pores (0.70 nm × 0.43 nm) (Fig. 5). The results of in situ UV/Vis spectroscopy and TGA of spent catalyst samples taken after TOS = 10.5 h indicated that no coke deposits were occluded in the channels of AlPO-41 (<0.2 wt.%), while significant coke deposits were formed on AlPO-34 (4.1 wt.%) and AlPO-18 (1.3 wt.%). According to the generally accepted reaction mechanism for strongly acidic MTO catalysts, aromatic and large olefinic hydrocarbon pool compounds are the key intermediates for the formation of light olefins. In the case of AlPO-41, the large one-dimensional pores (0.70 nm × 0.43 nm) and the very few Brønsted acid sites are not sufficient to stabilize catalytically active hydrocarbon pool compounds. As a result, no hydrocarbon pool compounds allowing the formation of light olefins could be detected on AlPO-41 by in situ UV/Vis spectroscopy and, therefore, DME is the dominant reaction product (Fig. 3).

^{1}H MAS NMR spectroscopic investigations revealed that the amount of accessible Brønsted acid sites on AlPO-34 (0.014 mmol/g) is higher than that on AlPO-18 (0.006 mmol/g). Comparing the MTO activity of AlPO-34 and AlPO-18, therefore, the amount of Brønsted

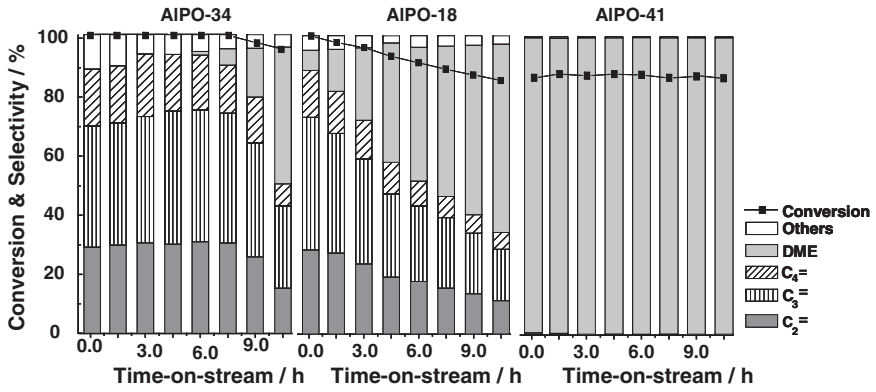

Fig. 3. Methanol conversion and product selectivity during the MTO conversion on the samples under study at 673 K and up to TOS = 10.5 h.

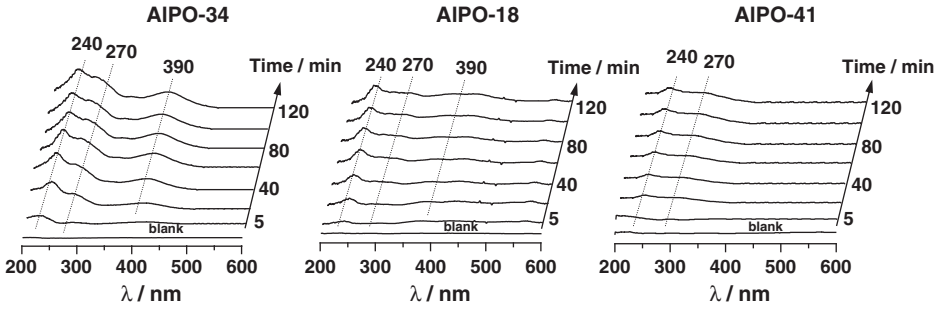

Fig. 4. In situ UV/Vis spectra recorded during the MTO reaction on the samples under study at 673 K and depicted as a function of the reaction time.

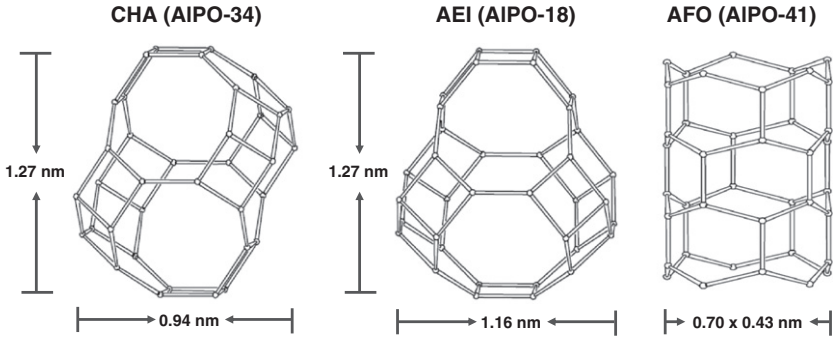

Fig. 5. Illustration of the framework structures of aluminophosphate samples employed in the present study for the MTO reaction.

acid sites play the key role in this process and better MTO performance is obtained over the catalyst with the larger number of Brønsted acid sites, i.e. over AlPO-34. For AlPO-41, the amount of accessible Brønsted acid sites (0.008 mmol/g) is higher than for AlPO-18, but no methanol conversion occurred over AlPO-41. This is caused by its larger one-dimensional pores, which are not sufficient to stabilize catalytically active hydrocarbon pool compounds (vide supra). Additionally, compared with SAPO-41, which has much more acid sites and exhibits good MTO conversion properties [19], AlPO-41 has only a few acid sites, and exhibits no MTO activity. In this case, the short contact time between reactants and Brønsted acid sites may be also a reason for the absence of any MTO conversion activity.

4. Conclusions

Low-silica aluminophosphates (AlPO-18, AlPO-34, AlPO-41) with small amounts of Brønsted acid sites and different framework topologies were synthesized and studied as catalysts for the MTO reaction. It is demonstrated that the Brønsted site density and framework topology of the aluminophosphates under study play vital roles in the MTO reaction. AlPO-18 and AlPO-34 with cages interconnected by 8-ring windows and traces of Brønsted acid sites are very active in the MTO conversion, while AlPO-41 with a similar Brønsted site density and one-dimensional 10-ring pores is inactive. For AlPO-34, a 100% methanol conversion with more than 90% selectivity to light olefins (C_1–C_4) were achieved and maintained for TOS = 7.5 h at the reaction temperature of 673 K. These results clearly indicate that the MTO reaction can be realized over aluminophosphate-type molecular sieves with a minimum number of Brønsted acid sites (0.006 to 0.014 mmol/g) and a suitable framework topology allowing the formation and stabilization of aromatic hydrocarbon pool compounds.

Acknowledgements

This work was supported by the National Basic Research Program of China (2009CB623502) and MOE (IRT0927).

Appendix A. Supplementary data

Supplementary data to this article can be found online at doi:10.1016/j.catcom.2011.09.025.

References

[1] M. Stöcker, Microporous and Mesoporous Materials 29 (1999) 3.
[2] Y. Wei, D. Zhang, F. Chang, Z. Liu, Catalysis Communications 8 (2007) 2248.
[3] W. Song, J.F. Haw, Angewandte Chemie International Edition 42 (2003) 892.
[4] R. Wendelbo, D. Akporiaye, A. Andersen, I.M. Dahl, H.B. Mostad, Applied Catalysis A 142 (1996) 197.
[5] Q. Zhu, J.N. Kondo, T. Tatsumi, S. Inagaki, R. Ohnuma, Y. Kubota, Y. Shimodaira, H. Kobayashi, K. Domen, Journal of Physical Chemistry C 111 (2007) 540.
[6] M.W. Anderson, B. Sulikowski, P.J. Barrie, J. Klinowski, Journal of Physical Chemistry 94 (1990) 2730.
[7] I.M. Dahl, S. Kolboe, Journal of Catalysis 161 (1996) 304.
[8] B. Arstad, S. Kolboe, Journal of the American Chemical Society 123 (2001) 8137.
[9] S. Svelle, F. Joensen, J. Nerlov, U. Olsbye, K.P. Lillerud, S. Kolboe, M. Bjørgen, Journal of the American Chemical Society 128 (2006) 14770.
[10] B.P.C. Hereijgers, F. Bleken, M.H. Nilsen, S. Svelle, K.-P. Lillerud, M. Bjørgen, B.M. Weckhuysen, U. Olsbye, Journal of Catalysis 264 (2009) 77.
[11] U. Olsbye, M. Bjørgen, S. Svelle, K.P. Lillerud, S. Kolboe, Catalysis Today 106 (2005) 108.
[12] S. Wilson, P. Barger, Microporous and Mesoporous Materials 29 (1999) 117.
[13] F.D.P. Mees, P.V.D. Voort, P. Cool, L.R.M. Martens, M.J.G. Janssen, A.A. Verberckmoes, G.J. Kennedy, R.B. Hall, K. Wang, E.F. Vansant, The Journal of Physical Chemistry. B 107 (2003) 3161.
[14] Q. Zhu, M. Hinode, T. Yokoi, M. Yoshioka, J.N. Kondo, T. Tatsumi, Catalysis Communications 10 (2009) 447.
[15] A. Tuel, S. Caldarelli, A. Meden, L.B. McCusker, C. Baerlocher, A. Ristic, N. Rajic, G. Mali, V. Kaucic, The Journal of Physical Chemistry. B 104 (2000) 5697.
[16] G. Poulet, A. Tuel, P. Sautet, The Journal of Physical Chemistry. B 109 (2005) 22939.
[17] Y.F. Ma, N. Li, S.H. Xiang, Microporous and Mesoporous Materials 86 (2005) 329.
[18] Y. Jiang, J. Huang, W. Dai, M. Hunger, Solid State Nuclear Magnetic Resonance 39 (2011) 116.
[19] W. Dai, X. Wang, G. Wu, N. Guan, M. Hunger, L. Li, ACS Catalysis 1 (2011) 292.
[20] Y. Jiang, J. Huang, V.R. Reddy Marthala, Y.S. Ooi, J. Weitkamp, M. Hunger, Microporous and Mesoporous Materials 105 (2007) 132.
[21] W. Dai, M. Scheibe, N. Guan, L. Li, M. Hunger, ChemCatChem 3 (2011) 1130.
[22] A.T. Aguayo, A.G. Gayubo, R. Vivanco, M. Olazar, J. Bilbao, Applied Catalysis A 283 (2005) 197.